Indo Global Journal of Pharmaceutical Sciences, 2018; 8(2): 55-61

INDO GLOBAL JOURNAL OF PHARMACEUTICAL SCIENCES
ISSN 2249- 1023

Solution Combustion Synthesis, Structural and Optical Properties of Dy^{3+} Doped $GdSrAl_3O_7$ Nanophosphor

Sonika Singh *, V.B. Taxak, S.P. Khatkar, Sheetal

Department of Chemistry, Maharshi Dayanand University, Rohtak-124001, India

Address for Correspondance
Sonika Singh,
sssonicasingh31@gmail.com

Received:
25.01.2018
Accepted:
28.01.2018

ABSTRACT: Single phased dysprosium doped $GdSrAl_3O_7$ nanophosphor has been successfully obtained via low temperature solution combustion synthesis (SCS). The crystal structure and particle morphology of the nanophosphor were investigated by the X-ray diffraction (XRD), Fourier transform infra-red spectroscopy (FT-IR), scanning electron microscopy (SEM) and transmission electron microscopy (TEM). All observations indicate that SCS yields pure-phased, well crystallized tetragonal $GdSrAl_3O_7$ phosphor with particle dimensions in the nano-regime at low sintering temperature (550°C). The photoluminescent excitation and emission spectra were studied to characterize the optical properties of the $GdSrAl_3O_7$: Dy^{3+} nanophosphor. Several sharp excitation peaks attributed to intra-4*f* transitions of the Dy^{3+} ions in the near UV region were observed, as well as characteristic blue and yellow emission ascribed to $^4F_{9/2} \rightarrow {}^6H_{15/2}$ and $^4F_{9/2} \rightarrow {}^6H_{13/2}$ transitions, respectively. The emission spectral features confirm that dysprosium occupies low symmetry site in $GdSrAl_3O_7$ lattice. In addition, the optimum Dy^{3+} ions concentration and decay curves were also investigated. The optical features suggest that Dy^{3+} doped $GdSrAl_3O_7$ nanophosphor may play a vital role in advanced lighting devices.

Cite this article as: Singh, S.; Taxak, V.B.; Khatkar, S.P.; Sheetal. Solution combustion synthesis, structural and optical properties of Dy3+ Doped GdSrAl3O7 nanophosphor. Indo Global J. Pharm. Sci., 2018; 8(2): 55-61.

Keywords Combustion; Optical; GdSrAl3O7: Dy3+; Nanophosphor.

INTRODUCTION

As important rare earth oxides, melilite complexes (ABC_3O_7) have been received considerable attention due to their stable structural features and high application potential in solid state laser materials, plasma display panels, mercury free- high discharge lamps (HID), high vision TV, plasma panel and scintillators [1-4]. The melilite ABC_3O_7 structure, where A is the rare earth elements, B is the alkaline earth elements and C is Al, Ga or In, is composed of eightfold coordinated alternating $(A/B)_2$ and corner–sharing tetrahedral anionic CO_4^{5-} layers. The trivalent A and divalent B cations occupy C_s symmetry sites while trivalent C cations are located at two non-equivalent tetragonal sites with S_4 and C_s symmetries. It has been found that the two dimensionally connected tetrahedral layered oxide network stabilizes oxygen by local relaxation, leading to high conductivity of interstitial oxide anions in the melilite lattice [5-7]. Up to now, various synthetic routes have been adopted to synthesize different RE^{3+} ions doped mellite oxide phosphors, including solid state method, sol-gel process and combustion approach [8-15]. As known, solid state process requires long sintering time (~24h) to increase diffusivity between precursor materials, resulting in agglomerated and coarse particles which adversely affect the efficiency of phosphor [8,16]. In sol-gel method, post sintering treatment at high temperature is needed to obtain the phosphor with single phase and high luminescence intensity [12]. In order to improve these drawbacks, solution combustion synthesis has been proved as an efficient, simple and self sustained process due to high reactivity of raw

materials at precursor level, which yields not only nano-sized oxide powders with large surface area but also allows homogenous doping of trace amounts of RE^{3+} ions in host lattice at low sintering temperature [17-19].

Among the melilite oxides, gadolinium strontium aluminate $GdSrAl_3O_7$ having tetragonal crystal structure with space group $P\text{-}42_1m$, could act as both efficient host lattice and sensitizer due to presence of Gd^{3+} as constituent ion, and offer excellent luminescent potentialities when doped with rare-earth ions (RE^{3+}) like other isostructural melilite oxides, $GdCaAl_3O_7$ and $GdSrGa_3O_7$ [8-11]. Recently, the doping of Tb^{3+} ions in $GdSrAl_3O_7$ lattice has been investigating by Zhou et. al. [10] via EDTA sol-gel process, reporting the pure melilite phase formation at higher sintering temperature (900°C) for 5h but luminescent properties of dysprosium ions in this host has not been studied so far. This paper reports an effective and rapid solution combustion approach for the first time synthesis of Dy^{3+} doped $GdSrAl_3O_7$ nanocrystalline phosphor at low temperature. The dopant Dy^{3+} ions has the well-known strong fluorescence in the visible spectral range around 480 nm and 570 nm ascribed to blue and yellow transitions from the $^7F_{9/2}$ state to $^7H_{15/2}$ and $^7H_{13/2}$ states, respectively. Dy^{3+} ions doped phosphor holds a great promise in white light emission by proper tuning of yellow to blue emission intensities on varying the composition of host [20-23]. Herein, the structural and photoluminescence features of Dy^{3+} doped $GdSrAl_3O_7$ nanophosphor with energy transfer mechanism from Gd^{3+} to Dy^{3+} ions were investigated in details.

MATERIALS AND METHODS

$Gd_{1-x}SrAl_3O_7$: xDy^{3+} nanopowders, where x = 1 to 15 mol% were synthesized using urea assisted solution combustion process. The chemical equation for the reaction was:

$$1\text{-}xGd(NO_3)_3 + xDy(NO_3)_3 + Sr(NO_3)_2 + 3Al(NO_3)_3 + 11.66CH_4N_2O \rightarrow Gd_{1-x}Dy_xSrAl_3O_7(s) + \text{gaseous products.}$$

According to stoichiometric composition $Gd_{1-x}Dy_xSrAl_3O_7$, high purity raw materials $Sr(NO_3)_2$, $Gd(NO_3)_3.6H_2O$, $Al(NO_3)_3$, $Dy(NO_3)_3.6H_2O$ and urea were dissolved in minimum quantity of deionized water. The amount of urea was calculated using total oxidizing and reducing valencies according to the concept used in propellant chemistry [24]. Finally the beaker containing the aqueous paste was placed in a preheated furnace maintained at 500°C. The mixture of metal nitrates (oxidizers) and fuel (urea) undergo rapid and self-sustaining combustion process and the chemical energy released during this exothermic redox reaction results in dehydration and foaming followed by decomposition. Consequently, the large amounts of volatile combustible gases generated alongwith flames, yields voluminous solid within 5-8 minutes. The foam thus obtained was again sintered at 550°C for 1h in order to eliminate unreacted nitrates, resulting in single phased dysprosium doped $GdSrAl_3O_7$ nanophosphor.

To reveal the crystalline phase of $Gd_{1-x}Dy_xSrAl_3O_7$ powders, X-ray diffraction (XRD) was carried out on Rigaku Ultima-IV X-ray powder diffractometer at 40 kV tube voltage and 40 mA tube current with CuKα radiation in the 2θ ranging from15 to 70°. The functional groups in $GdSrAl_3O_7$ lattice were identified by the Fourier transform infra-red spectroscopy (Perkin-Elmer spectrometer) in the spectral range 4000-400cm^{-1}. The morphology and particle size were evaluated using scanning electron microscopy (SEM) on Jeol JSM-6510 and transmission electron microscopy (TEM) on Hitachi F-7500. The photoluminescence excitation and emission spectra of the nanophosphor in the ultraviolet-visible region and decay curves under time scan-mode were analyzed by fluorescence spectrophotometer (Hitachi F-7000) equipped with Xe-lamp as the light source.

RESULTS AND DISCUSSION

Structural studies

$GdSrAl_3O_7$ is one of the complex oxide of melilite family, consisting of tetragonal crystals with the space group $P\text{-}42_1m$ and lattice parameter a = 7.801A° and c = 5.132A°. The $GdSrAl_3O_7$ lattice is built up of AlO_4^{5-} tetrahedral layers and the Sr^{2+} and Gd^{3+} ions are randomly distributed in between the layers at C_s symmetry sites. The XRD patterns of $Gd_{0.90}Dy_{0.10}SrAl_3O_7$ nanophosphor, as-synthesized (500°C) and sintered (550°C, 1h) along with standard data of melilite oxide, $GdSrAl_3O_7$ (JCPDS No. 50-1817) are presented in Fig. 1. In the as-synthesized sample, diffraction peaks at 16.09 (001), 17.30 (111), 23.94 (111), 25.65 (210), 28.84 (201), 31.04 (211), 35.09 (002), 36.50 (310), 43.89 (212) and 51.46 (312) belonging to tetragonal phased $GdSrAl_3O_7$ (JCPDS No. 50-1817) with a shoulder peak marked as '*' at 19.8° due to unreacted nitrates were observed.

It is quite visible that the sintering of $Gd_{0.90}Dy_{0.10}SrAl_3O_7$ powder at 550°C does not induce any significant phase change so far except the impurity peak gets disappeared completely. The XRD patterns indicate that well-crystallized melilite phased $GdSrAl_3O_7$: Dy^{3+} nanophosphor could be easily obtained under the low temperature synthetic conditions. Hence, it is very easy to conclude that SCS is an effective

approach which allows homogenous mixing of different oxidizers (i.e. metal nitrates) at molecular level during pre-sintering process due to self sustained combustion of metal nitrate and an organic fuel at low furnace temperature (500°C).

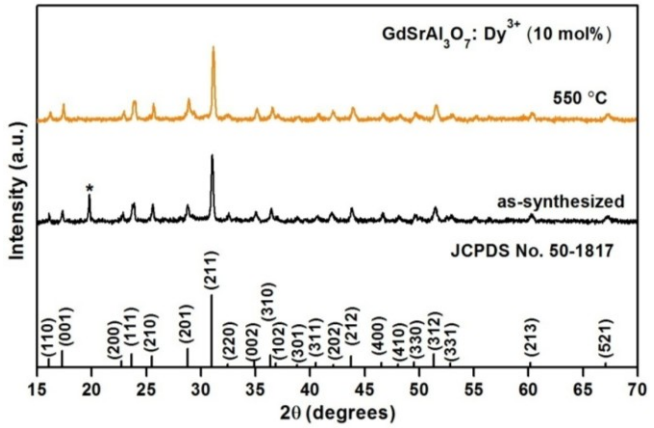

Fig. 1 XRD patterns of $Gd_{0.90}$ $Dy_{0.10}SrAl_3O_7$ nanophosphor, as-synthesized and sintered at 550°C along with standard data of $GdSrAl_3O_7$ (JCPDS No. 50-1817).

The XRD profiles of $Gd_{1-x}Dy_xSrAl_3O_7$ nanophosphors doped with different dysprosium contents, sintered at 550°C alongwith standard reference data (JCPDS No. 50-1817) are depicted in Fig. 2. The well defined diffraction peaks confirmed that, after sintering at 550°C, powder samples crystallize in a pure tetragonal $GdSrAl_3O_7$ phase (JCPDS No. 50-1817). It also implies that the incorporation of Dy^{3+} ions does not cause any distortion in the melilite lattice as Dy^{3+} ions (R_{Dy3+} = 0.97 A°) can easily enter into C_s symmetry sites for substituting Gd^{3+} ions (R_{Gd3+} =1.00 A°) in $GdSrAl_3O_7$.

The average particle size, D of $Gd_{1-x}Dy_xSrAl_3O_7$ powders, was determined from the XRD parameters according to Scherrer's equation $D = 0.941\lambda/\beta \cos\theta$, where λ is the wavelength of CuKα radiation (0.1548 nm), β is the full width in radians at half-maximum (FWHM) and θ is the Bragg's angle of an observed X-ray diffraction peak. From the FWHM value of the most intense peak (211), the calculated particle size corresponding to 1, 5, 10 and 15 mol% of Dy^{3+} ions in $Gd_{1-x}SrAl_3O_7$ powder, sintered at 550°C came out to be 49 nm, 48 nm, 45 nm and 42 nm, respectively. Within all samples, the average size standard deviation was 45 ± 4 nm, indicating that the amount of Dy^{3+} ions has no remarkable influence on the particle size of $Gd_{1-x}Dy_xSrAl_3O_7$ nanophosphor.

The morphological features of $Gd_{0.90}Dy_{0.10}SrAl_3O_7$ nanophosphor, sintered at 550°C were investigated by scanning electron microscopy and transmission electron microscopy. SEM image of $Gd_{0.90}Dy_{0.10}SrAl_3O_7$ nanophosphor depicts smooth and densely packed tetragonal porous particles, as expected arise from the non-uniform distribution of temperature and mass flow in the combustion flame (Fig. 3).

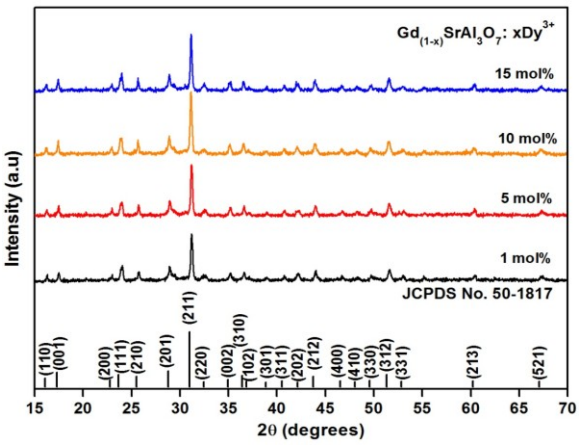

Fig. 2 XRD patterns of $Gd_{1-x}Dy_xSrAl_3O_7$ nanophosphors doped with different dysprosium contents, sintered at 550°C alongwith standard data of $GdSrAl_3O_7$ (JCPDS No. 50-1817).

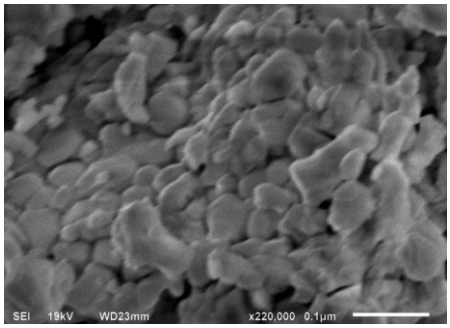

Fig.3 SEM image of $Gd_{0.90}Dy_{0.10}SrAl_3O_7$ nanophosphor, sintered at 550°C.

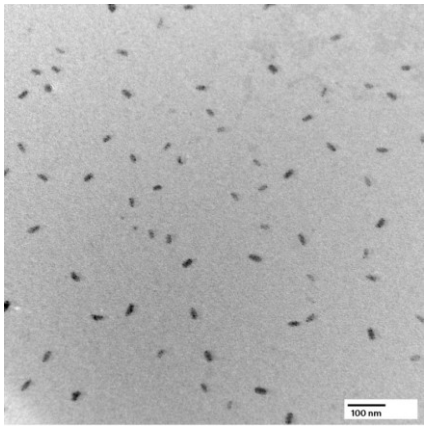

Fig.4 TEM image of $Gd_{0.90}Dy_{0.10}SrAl_3O_7$ nanophosphor, sintered at 550°C.

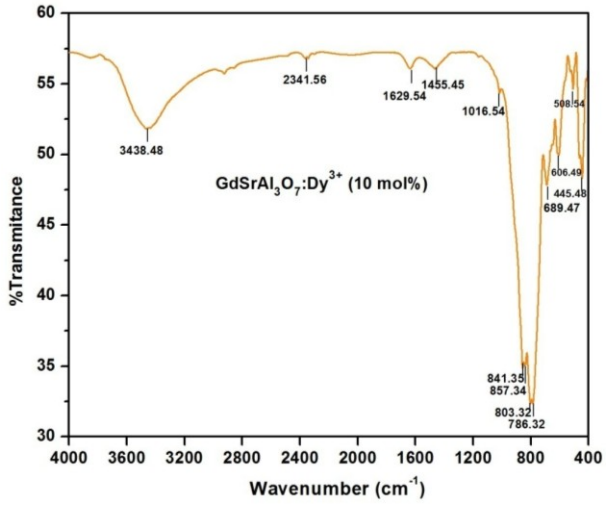

.

Fig.5 FT-IR spectrum of $Gd_{0.90}Dy_{0.10}SrAl_3O_7$ nanophosphor, sintered at 550°C.

The combustion derived products with high surface area and porous network are believed to be an outcome of large amount of escaping gaseous materials during the self-sustained combustion process [25-26]. TEM image of $Gd_{0.90}Dy_{0.10}SrAl_3O_7$ nanophosphor sintered at 550°C, shows monodispersed tetragonal shaped particles with sizes in 40-50 nm range (Fig. 4). The average particles size estimation of $Gd_{0.90}Dy_{0.10}SrAl_3O_7$ nanophosphor is consistent with that determined from the XRD patterns.

The FT-IR spectrum of $Gd_{0.90}Dy_{0.10}SrAl_3O_7$ nanophosphor, sintered at 550°C in the frequency region of 4000-400cm^{-1} is depicted in Fig. 5. Modes in the lower region (1000-400 cm^{-1}) are assigned to the aluminum-oxygen stretching and bending vibrations of AlO_4^{5-} tetrahedron and other metal-oxygen bonds present in the melilite structure. In addition, absorption bands related to characteristics H-O-H bending vibrations of absorbing free H_2O (1630 cm^{-1}) and O-H stretching vibration (3438 cm^{-1}) also appeared in the sample. It is significant to note that the fundamental residual NO_3^- peak around 1384 cm^{-1} was not detected in the spectrum, confirming the formation of impurity free pure melilite phased structure at low crystallization temperature.

Optical studies

The photoluminescence excitation (PLE) spectrum of $Gd_{0.90}Dy_{0.10}SrAl_3O_7$ nanophosphor, sintered at 550°C, monitored with 574 nm ($^4F_{9/2} \rightarrow {}^6H_{13/2}$) as emission wavelength is illustrated in Fig. 6. The excitation spectrum monitored at yellow emission consists of several characteristic sharp peaks corresponding to intra-4*f* transitions of Gd^{3+} and Dy^{3+} in the melilite host. Among these excitations, the peaks at 274 nm and 312 nm are assigned to transitions of Gd^{3+} ions from $^8S_{7/2}$ state to $^6I_{7/2}$ and $^6P_{7/2}$ states while the peaks in the 320 -500 nm correspond to *f–f* transitions of Dy^{3+} ions within its $4f^9$ configuration. These excitation peaks in longer wavelength region at 322 nm, 350 nm, 385 nm, 423 nm, 452 nm and 463 nm are ascribed to $^6H_{15/2} \rightarrow {}^6P_{3/2}$, $^6H_{15/2} \rightarrow {}^6P_{7/2}$, $^6H_{15/2} \rightarrow {}^4I_{13/2}$, $^6H_{15/2} \rightarrow {}^4G_{11/2}$, $^6H_{15/2} \rightarrow {}^4I_{15/2}$ and $^6H_{15/2} \rightarrow {}^4F_{9/2}$ transitions, respectively of Dy^{3+} ions in $GdSrAl_3O_7$ lattice [27]. The host or $Dy^{3+} \rightarrow O^{2-}$ charge sensitized luminescence was not observed in the short wavelength region indicating weak Dy^{3+} ions interactions with melilite host while presence of dominant $^8S_{7/2} \rightarrow {}^6I_{7/2}$ and $^8S_{7/2} \rightarrow {}^6P_{7/2}$ electronic transitions of Gd^{3+} ions in the spectrum confirms the efficient energy transfer between Gd^{3+} and Dy^{3+} ions in host lattice [28-29].

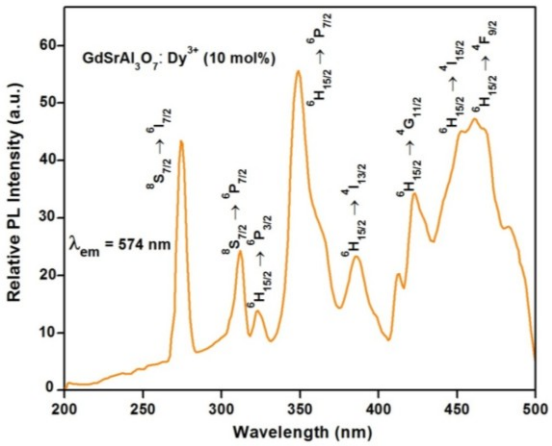

Fig.6 Photoluminescence excitation (PLE) spectrum of $Gd_{0.90}Dy_{0.10}SrAl_3O_7$ nanophosphor, sintered at 550°C, monitored with λ_{em} = 574 nm.

The photoluminescence (PL) spectra of $Gd_{0.90}Dy_{0.10}SrAl_3O_7$ nanophosphor as-synthesized and sintered at 550°C, monitored with 350 nm ($^6H_{15/2} \rightarrow {}^6P_{7/2}$) as excitation wavelength in 400-650 nm region is depicted in Fig. 7. The two main emission bands in the 450-500 nm (blue region) and 550-600 nm (yellow region) corresponding to transitions between well-defined 4*f* energy states of the Dy^{3+} ions were observed. The blue emission containing multiple emission lines, centered at 478 nm and dominating yellow emission centered at 574 nm are assigned to $^4F_{9/2} \rightarrow {}^6H_{15/2}$ and $^4F_{9/2} \rightarrow {}^6H_{13/2}$ transitions of Dy^{3+} ions, respectively. With respect to Dy^{3+} ions, magnetic allowed dipole $^4F_{9/2} \rightarrow {}^6H_{15/2}$ transition gets hardly influenced by the crystal field symmetry of dysprosium ions while forced electric allowed transition $^4F_{9/2} \rightarrow {}^6H_{13/2}$ being hypersensitive appreciably affected by chemical surrounding of the luminescent center [30]. Both samples exhibits stronger forced electric transition (yellow emission) than magnetic dipole transition (blue emission) as there is a high probability of substitution of Dy^{3+} ions into low inversion symmetric Gd sites (C_s) in this melilite oxide due to comparable size of Dy^{3+} and Gd^{3+} ions.

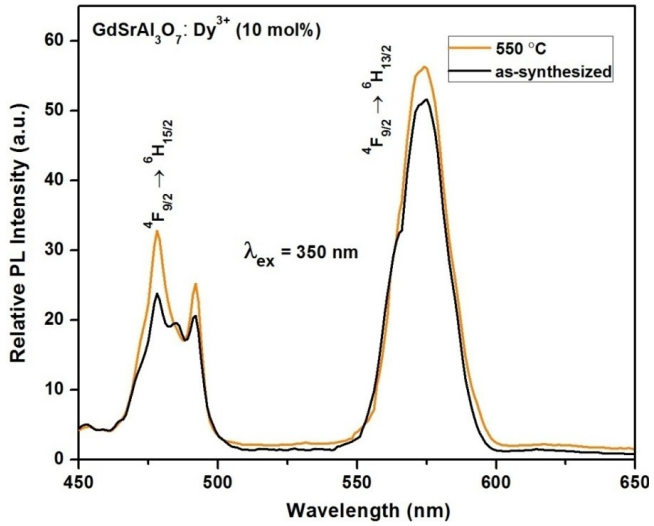

Fig.7 Photoluminescence (PL) spectrum of $Gd_{0.90}Dy_{0.10}SrAl_3O_7$ nanophosphor as-synthesized and sintered at 550°C, monitored with λ_{em} = 350 nm.

However, the PL spectrum of as-synthesized $Gd_{1.90}SrDy_{0.10}Al_3O_7$ nanophosphor shows slightly weak emission with maintained shape and positions of peaks corresponding to both transitions as compared to that of sample, sintered at 550°C (1h). This indicates that $Gd_{1.90}SrDy_{0.10}Al_3O_7$ nanophosphors are not well crystallized at 500°C due to presence of surface impurities in host lattice which may be omitted out after sintering, leading to improvement in crystallinity as confirmed by the XRD measurements.

The PL spectra of $Gd_{1-x}Dy_xSrAl_3O_7$ nanophosphors, sintered at 550°C with dysprosium doping contents ranging from 1 to 15 mol%, monitored with 350 nm as excitation wavelength are shown in Fig. 8. For all $Gd_{1-x}Dy_xSrAl_3O_7$ samples, the hypersensitive yellow ($^4F_{9/2}\rightarrow{}^6H_{13/2}$) emission of Dy^{3+} ions is the prominent one as Dy^{3+} ions preferentially substitutes low symmetry Gd^{3+} sites (C_s) with no inversion center in $GdSrAl_3O_7$ lattice. The relative PL intensities corresponding to both yellow and blue emission enhanced with the increasing concentration of Dy^{3+} ions, reaching the maximum at 10 mol% of dysprosium contents while decreased with the further increase of dopant concentration. Such behavior is due to cross-relaxation mechanism between luminescent centers, caused by quenching of the energy state $^4F_{9/2}$ at higher dysprosium contents via non-radiative energy transfer process such as;

$$Dy^{3+}(^4F_{9/2}) + Dy^{3+}(^6H_{15/2}) \rightarrow Dy^{3+}(^4F_{9/2}/{}^6H_{7/2}) + Dy^{3+}(^6F_{3/2})$$

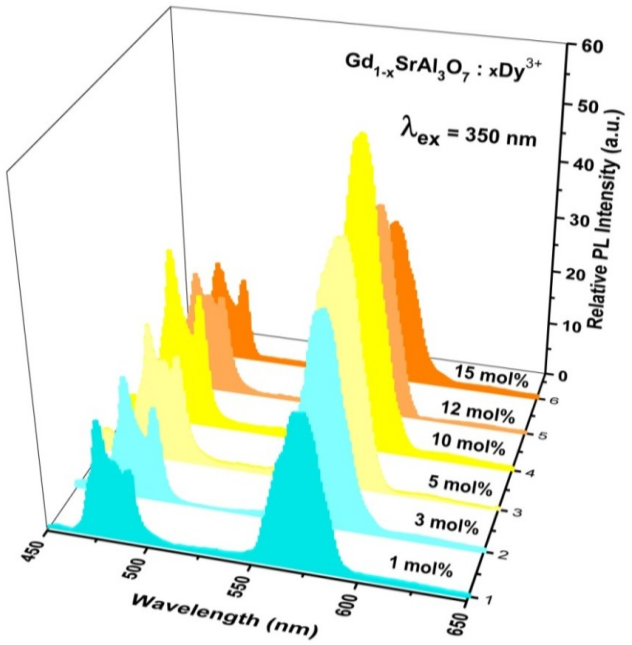

Fig. 8 Photoluminescence spectra of $Gd_{1-x}Dy_xSrAl_3O_7$ nanophosphors doped with different dysprosium contents, sintered at 550°C and monitored with λ_{em} = 350 nm.

It has been noticed that value of yellow to blue emission ratio (Y/B ~1.7) does not show significant changes with the increasing Dy^{3+} contents in $GdSrAl_3O_7$ host, indicating hypersensitive electric forced transition ($^4F_{9/2}\rightarrow{}^6H_{13/2}$) senses same crystal field environment at Dy^{3+} symmetry sites in $GdSrAl_3O_7$ lattice at different doping concentrations.

The luminescence decay curves corresponding to $^4F_{9/2} \rightarrow {}^6H_{13/2}$ transition at 574 nm for $Gd_{1-x}Dy_xSrAl_3O_7$ nanophosphors in terms of Dy^{3+} ions concentrations, monitored with 350 nm excitation wavelength are shown in Fig. 9. In all samples, $^4F_{9/2}\rightarrow{}^6H_{13/2}$ transitions show single exponential behavior, represented by the equation $I = I_0 \exp(-t/\tau)$, where τ is the radiative decay time, I and I_0 are the luminescence intensities at time t and 0, respectively. The calculated lifetimes are 2.61, 2.43, 2.41, 2.39, 2.33 and 1.69 for 1, 3, 5, 10, 12 and 15 mol% of Dy^{3+} ions, respectively in $Gd_{1-x}SrAl_3O_7$ nanophosphors. At higher concentration, the distance between the dysprosium ions shortens subsequently non-radiative energy transfer between optical active ions become more frequent, hence life time decreases with the increasing dopant concentration.

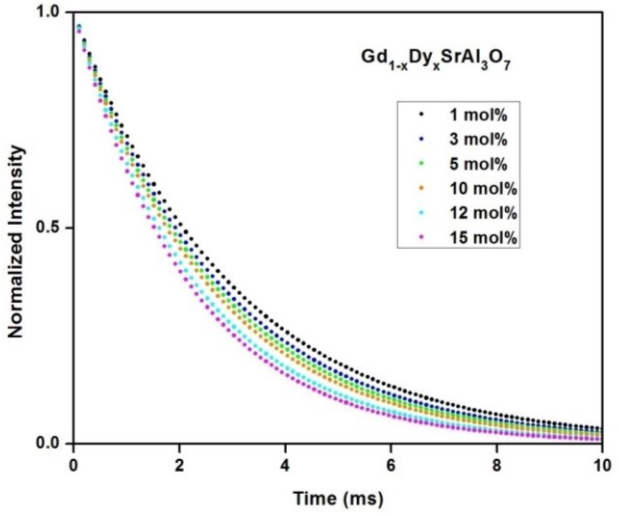

Fig.9 Decay curves of $Gd_{1-x}Dy_xSrAl_3O_7$ nanophosphors doped with different Dy^{3+} contents, sintered at 550°C and monitored with λ_{ex} = 350 nm

As stated earlier, shape of emission curves and Y/B ratio does not vary much over the range of dysprosium contents in $GdSrAl_3O_7$, hence the Commission International De I'Eclairage chromaticity coordinates corresponding to different concentrations of dysprosium fall in yellowish-white region, with color coordinates of x =0.361 and y = 0.436 for $Gd_{0.90}Dy_{0.10}SrAl_3O_7$ nanophosphor, sintered at 550°C which is found to be better than that of other reported Dy^{3+} doped phosphor such as Gd_2O_3: Dy^{3+} (0.41, 0.44) phosphor [31].

CONCLUSION

In Summary, highly crystalline melilite phased $GdSrAl_3O_7$: Dy^{3+} nanophosphor has been successfully synthesized by low cost solution combustion approach at sintering temperature, 550°C as confirmed by the XRD patterns. Morphological studies reveal that uniform tetragonal particles with narrow size distribution could be obtained by this low temperature method. Optical studies of Dy^{3+} doped $GdSrAl_3O_7$ nanophosphor were studied in details. The PL spectra exhibits stronger yellow emission ($^4F_{9/2} \rightarrow {}^6H_{13/2}$) as compared to blue emission ($^4F_{9/2} \rightarrow {}^6H_{15/2}$) under excitation at 350 nm, confirming that Dy^{3+} preferably substituted low symmetry Gd^{3+} sites in the melilite lattice. An efficient energy transfer from the Gd^{3+} to Dy^{3+} ions can be achieved. Luminescent analysis reveal that the optimum Dy^{3+} concentration is around 10 mol% and non-radiative cross-relaxation process between neighboring Dy^{3+} ions might be responsible for the concentration quenching phenomenon in this potential luminescent nanomaterial.

REFERENCES

1. N. Kodama, Y. Tanii, M. Yamaga, "Optical properties of long-lasting phosphorescent crystals Ce^{3+} doped $Ca_2Al_2SiO_7$ and $CaYAl_3O_7$", Journal of Luminescence 87 (2000) 1076-1078.
2. S. Kubota, M. Izumi, H. Yamane, M. Shimada, "Luminescence of Eu^{3+}, Tb^{3+} and Tm^{3+} in $SrLaGa_3O_7$", Journal of Alloys and Compounds 283 (1999) 95-101.
3. M.A. Kale, C.P. Joshi, S.V. Moharil, P.L. Muthal, S.M. Dhopte, "Luminescence in $LaCaAl_3O_7$ prepared by combustion synthesis", Journal of Luminescence 128 (2008) 1225-1228.
4. M. Malinowski, I. Pracka, P. Myziak, R. Piramidowicz, W. Wolinski, "Spectroscopy of Dy^{3+}-doped $SrLaGa_3O_7$ crystals", Journal of Luminescence 72 (1997) 224.
5. W.R. Romanowski, S. Golab, W.A. Pisarski, G.D. Dzik, M. Berkowski, A. Pajaczkowska, "Growth and characterization of new disordered crystals for the design of all solid state lasers", International Journal of Electronics 81(1996) 457-465.
6. M. Karbowiak, P. Gnutek, C. Rudowicz, W.R. Romanowski, "Crystal-field analysis for RE^{3+} ions in laser materials: II. Absorption spectra and energy levels calculations for Nd^{3+} ions doped into $SrLaGa_3O_7$ and $BaLaGa_3O_7$ crystals and Tm^{3+} ions in $SrGdGa_3O_7$", Chemistry Physics 387 (2011) 69-78.
7. B. Liu, D. Ding, Z. Liu, F. Chen, C. Xia, Synthesis and electrical conductivity of various melilite-type electrolytes $Ln_{1+x}Sr_{1-x}Ga_3O_{7+x/2}$", Solid State Ionics 191 (2011) 68.
8. X. Zhang, J. Zhang, L. Liang, Q. Su "Luminescence of $SrGdGa_3O_7$: RE^{3+} (RE = Eu, Tb) phosphors and energy transfer from Gd^{3+} to RE^{3+}", Material Research Bulletin 40 (2005) 281-288.
9. L. Zhou, W.C.H. Choy, J. Shi, M. Gong, H. Liang, T.I. Yuk, "Synthesis, vaccum ultraviolet and near ultraviolet-excited luminescent properties of $GdCaAl_3O_7$: RE^{3+} (RE = Eu, Tb) ", Journal of Solid State Chemistry 178 (2005) 3004 -3009.
10. L. Zhou, W.C.H. Choy, J. Shi, M. Gong, H. Liang, "Synthesis and luminescent properties of $GdSrAl_3O_7$:Tb^{3+} phosphor under VUV/UV excitation", Journal of Alloys and Compounds 463 (2008) 302.
11. J.G. Mahakhode, S.J. Dhoble, C.P. Joshi, S.V. Mohari, "Combustion synthesis of phosphors for plasma display panels", Journal of Alloys and Compounds. 438 (2007) 293.
12. A. Bao, H. Yang, C. Tao, "Synthesis and luminescent properties of nanoparticles $LaSrAl_3O_7$:Eu, Tb", Current Applied Physics 9 (2009) 1252-1256.
13. V. Singh, V.V.R.K. Kumar, R.P.S. Chakradhar, H.Y. Kwak, "Synthesis, characterization and photoluminescence of Eu^{3+}, Ce^{3+} co-doped $CaLaAl_3O_7$ phosphors", Philosophical Magazine 90 (2010) 3095-3105.
14. Sheetal, V.B. Taxak, Mandeep, S.P. Khatkar, "Synthesis, characterization and luminescent properties of Eu/Tb-doped $LaSrAl_3O_7$", Journal of Alloys and Compounds 549 (2013) 135-140.
15. V. Singh, S. Watanabe, T.K. Gundurao, H.Y. Kwak "Synthesis, characterization, luminescence and defect centres in $CaYAl_3O_7$: Eu^{3+}", Journal of Fluorescence 21 (2011) 313-320.
16. P.S. Anil Kumar, J.J. Shrotri, S.D. Kulkarni, C.E. Deshpande, S.K. Date, "Low temperature synthesis of Ni0.8Zn0.2Fe2O4 powder and its characterization", Materials. Letters 27(1996) 293.
17. S.T. Aruna, A.S. Mukasyan, "Combustion synthesis and nanomaterials", Current Opinion in Solid State Material Science 12 (2008) 44.
18. L.G. Jacobsohn, B.L. Bennett, R.E. Muenchausen, J.F. Smith, D.W. Cooke, "Luminescent properties of nanophosphors", Radiation Measurement 42 (2007) 675-678.

19. V. Singh, V.K. Rai, K.A. Shamery, J. Nordmann, M. Hasse "NIR to visible upconversion in Er^{3+}/ Yb^{3+} co-doped $CaYAl_3O_7$ phosphor obtained by solution combustion process", Journal of Luminescence 131(2011) 2679-2682.
20. R. Zhang, X. Wang, "Preparation and luminescent characteristics of $Sr_3RE_2(BO_3)_4$: Dy^{3+} (RE = Y, La, Gd) phosphors for white LED", Journal of Alloys and Compounds 509 (2011) 1197.
21. L. Cheng, X. Li, J. Sun, H. Zhong, Y. Tian, J. Wan, "Investigation of the luminescence properties of Dy^{3+}-doped α-$Gd_2(MoO_4)_3$ phosphors", Physics B: Condensed Material. 405 (2010) 4457.
22. X. Zhang, H.J. Seo, "Luminescence properties of novel Sm^{3+}, Dy^{3+} doped $LaMoBO_6$ phosphors", Journal of Alloys and Compounds 509 (2011) 2007.
23. Q. Su, Z. Pei, L. Chi, H. Zhang, Z. Zhang, F. Zou, "The yellow-to-blue intensity ratio (Y/B) of Dy^{3+} emission", Journal of Alloys and Compounds 192 (1993) 25.
24. S. Ekambaram, M. Maaza, K.C. Patil, "Synthesis of lamp phosphors: facile combustion approach", Journal of Alloys and Compounds 93 (2005) 81-92.
25. V. Singh, S. Watanabe, T.K. GunduRao, H.Y. Kwak, "Luminescence and defect centres in Tb^{3+} doped $LaMgAl_{11}O_{19}$ phosphors", Solid State Sci. 12, 1981 (2010)
26. S.S. Pitale, V. Kumar, I. Nagpure, O.M. Ntwaeaborwa, H.C. Swart, "Luminescence investigations on $LiAl_5O_8$:Tb^{3+} nanocrystalline phosphors", Current Applied Physics 11(2011) 341.
27. B. Tian, B. Chen, Y. Tian, J. Sun, X. Li, J. Zhang, H. Zhong, L. Cheng, R. Hua, "Concentration and temperature quenching mechanisms of Dy^{3+} luminescence in $BaGd_2ZnO_5$ phosphors", Journal of Physics Chemistry Solids 73 (2012) 1314-1319.
28. G.S. Rama Raju, J.Y. Park, H.C. Jung, B.K. Moon, J.H.Jeong, J.H. Kim, "Luminescence properties of Dy^{3+} :$GdAlO_3$nanopowder phosphors", Current Applied Physics 9(2009) e92-e9.
29. X. Zhang, H.J.Seo, "Luminescence properties of novel Sm^{3+}, Dy^{3+} doped $LaMoO_6$ phosphors", Journal of Alloys and Compounds 509 (2011) 2007-2010.
30. L.A. Diaz-Torres, E.D.L Rosa, P. Salas, V.H. Romero, A. Angeles-Chavez, "Efficient photoluminescence of Dy^{3+} at low concentrations on nanocrystalline ZrO_2", Journal of Solid State Chemistry 181(2008) 75-80
31. P. Lingling, H. Tao, C. Hui, Z. Tiejun, "Spectroscopic properties of Gd_2O_3: Dy^{3+} nanocrystals" Journal of Rare Earths, 31(2013) 235.

Indo Global Journal of Pharmaceutical Sciences(ISSN 2249 1023 ; UGC Journal No.: 44477; CODEN- IGJPAI; NLM ID: 101610675) indexed and abstracted in EMBASE(Elsevier), UGC Journal List, National Library of Medicine (NLM) Catalog, Elsevier(EMBASE), ResearchGate, Publons, CAS (ACS), Index Copernicus, Google Scholar and many more. For further details, visit http://iglobaljournal.com